Aeronautical Channel Characterization

PHILLIP A. BELLO

Abstract—This paper is concerned with characterizing the link between an airplane and a satellite. Attention is focused on the effect of indirect paths scattered from the surface of the earth. Applicable propagation-theoretic and system function-theoretic work is reviewed and integrated. Some new and some known expressions for channel correlation functions are presented for the "steepest descent" channel model.

I. Introduction

THE aeronautical communication channel appears in a multiplicity of command and control and communication systems; military, nonmilitary, and civilian. We shall not get involved in a discussion of these various systems which, moreover, have been fairly well covered elsewhere in this issue. Rather we shall focus on the kinds of communication links involved and single out for discussion one particular type of link that is of major importance in advanced aeronautical communications.

One may categorize the links involved in aeronautical communications on the basis of terminal locations as: 1) air-air; 2) air-ground; 3) air-space; and 4) ground-space links. In studying the modeling of these links it becomes evident that they are conveniently (although approximately) decomposable into combinations of propagation channels that exhibit certain characteristic propagation effects to the exclusion of others. For the purposes of the present discussion we identify five propagation channels, namely the 1) surface scatter; 2) ionospheric scintillation; 3) tropospheric refraction; 4) line-of-sight tropospheric scatter; and 5) ionospheric refraction (HF). Other propagation channels may be defined but these five appear adequate to characterize aeronautical communication channels.

The channel of major importance in satellite-based air traffic control systems is the surface scatter channel. Due to space limitations it was decided to concentrate on this channel alone for this paper. Also, consideration will be given only to the fading dispersive characteristics of this channel. Section II reviews briefly the mathematical tools that have become useful in modeling the input-output behavior of time-variant linear channels, including system functions, channel correlation functions, and statistics. Following this, Section III discusses the characteristics of the surface scatter channel. The material is divided into two parts, one dealing with propagation physics results (e.g., scattering cross sections) and the other dealing with system function characteristics (e.g., Doppler power spectrum, delay power spectrum).

II. System Function Characterization of Random Time-Variant Channels

The propagation channels of interest here are linear and their behavior may be described on an "instantaneous" input-output basis with the aid of system functions as discussed in Section II-A. Section II-B introduces channel correlation functions to provide the simplest second-order statistical description of these channels on a quasi-stationary basis. To obtain estimates of error rates in data transmission some assumption must be made about probability distributions of channel fluctuations. Section II-C summarizes the various statistical channel models that have been useful in this regard.

A. System Functions

There exists a variety of system functions for characterizing the input-output behavior of linear time-varying systems. The most general discussion of these system functions and their relationships has been presented in [1]. For the purposes of the present brief discussion it is sufficient to confine attention to the time-variant transfer function $T(f, t)$ and the time-variant impulse response $g(t, \xi)$.[1] For simplicity of presentation we shall use complex envelope representation throughout. Thus the input signal would be represented by the complex signal $z(t)$. The real signal would be a narrow-band process with envelope $|z(t)|$ and with phase $\measuredangle z(t)$ measured with respect to carrier phase $2\pi f_0 t$, where f_0 is the carrier frequency.

In complex notation the input-output relationships corresponding to the use of $T(f, t), g(t, \xi)$ are

$$w(t) = \int Z(f)T(f, t) \exp(j2\pi ft)\, df \tag{1}$$

$$w(t) = \int z(t - \xi)g(t, \xi)\, d\xi, \tag{2}$$

where $w(t)$ is the output signal (complex) and $Z(f)$ the spectrum of $z(t)$.

The transfer function $T(f, t)$ and impulse response $g(t, \xi)$ are Fourier transform pairs,

$$T(f, t) = \int g(t, \xi) \exp(-j\,2\pi f\xi)\, d\xi \tag{3}$$

$$g(t, \xi) = \int T(f, t) \exp(j\,2\pi f)\, d\xi. \tag{4}$$

It is readily seen that the time-variant transfer function at the frequency f (actually f hertz away from carrier frequency f_0) is just equal to the complex modulation observed on a re-

[1] A third system function that the author has found useful is the delay spread function $U(\xi, \nu)$ [1], which provides the input-output relationship

$$w(t) = \iint z(t - \xi) \exp(j\,2\pi\nu t)U(\xi, \nu)\, d\xi\, d\nu.$$

This system function represents the time-variant channel as a continuum of delay and Doppler shifts with complex gain $U(\xi, \nu)\, d\xi\, d\nu$ for the delay ξ and Doppler shift ν. $U(\xi, \nu)$ is the Fourier transform of $g(t, \xi)$ over the t variable. It is also the double Fourier transform of the time-variant transfer function $T(f, t)$.

Manuscript received October 26, 1972.
The author is with CNR, Inc., Newton Upper Falls, Mass. 02164.

ceived RF carrier transmitted at $f_0 + f$ hertz. Thus the time-varying envelope of this received carrier is $|T(f, t)|$ and the time-varying phase of this received carrier measured with respect to the input carrier phase is $\measuredangle T(f, t)$.

While $g(t, \xi)$ may be described formally as the response at time t to an impulse input at $t - \xi$, the author has found it much more useful in modeling radio channels to regard $g(t, \xi)$ as the differential complex time-varying gain associated with path delays in the delay interval $(\xi, \xi + d\xi)$ in a differential tapped delay line interpretation of (2).

With the use of delta functions the previous integral formulations include as a special case the idealized radio channel consisting of a finite number K of discrete paths, i.e..

$$g(t, \xi) = \sum_{k=1} G_k(t)\delta(\xi - \xi_k) \tag{5}$$

for which (2) and (3) become

$$w(t) = \sum_{k=1}^{K} G_k(t)z(t - \xi_k) \tag{6}$$

$$W(f) = \sum_{k=1}^{K} G_k(t) \exp(-j 2\pi f \xi_k). \tag{7}$$

The tapped delay line interpretation of $g(t, \xi)$ is particularly evident in (5)-(7).

The discrete model is particularly useful in modeling the ionospheric and tropospheric refraction channels. The integral formulation is appropriate for scatter channels, such as the scatter portions of the line-of-sight tropospheric scatter and surface scatter channels.

Because of its frequent occurrence in radio channel modeling we mention here the special mixed case of a single path combined with a continuum of paths, i.e.,

$$g(t, \xi) = G(t)\delta(\xi - \xi_0) + \hat{g}(t, \xi). \tag{8}$$

The ionospheric scintillation, line-of-sight tropospheric scatter, and surface scatter channels require such a mixed description.

B. Correlation Functions

While the fluctuations in radio channels are due to nonstationary statistical phenomena, on a short enough time scale and for small enough bandwidths the fluctuations in time and frequency can be approximately characterized as statistically stationary. For want of a better word this approximate stationarity is called quasi-stationarity. A mathematical basis for defining quasi-stationary radio channels is presented in [1].

When the time variant transfer function is idealized to have stationary fluctuations in time and frequency the channel is said to be [1] wide-sense-stationary uncorrelated scattering (WSSUS). For the WSSUS channel

$$\overline{T^*(f, t)T(f + \Omega, t + \tau)} = R(\Omega, \tau), \tag{9}$$

i.e., the cross-correlation function between the complex envelopes of received carriers transmitted Ω hertz apart is dependent only on the frequency separation Ω and time lag τ. The function $R(\Omega, \tau)$ is called the "time-frequency correlation function."

Because of the Fourier transform relationship between $T(f, t)$ and $g(t, \xi)$ one may show that (9) implies

$$\overline{g^*(t, \xi)g(t + \tau, \eta)} = Q(\tau, \xi)\delta(\eta - \xi) \tag{10}$$

where $\delta(\cdot)$ is the unit impulse function and $Q(\tau, \xi)$ is the Fourier transform of $R(\Omega, \tau)$ on the Ω variable. $Q(\tau, \xi)$ has been called the "tap gain correlation function" because it is proportional to the autocorrelation function of the fluctuations in the complex tap gain at delay ξ in the differential tapped delay line model interpretation of (2). Equation (10) implies that the fluctuations of the complex gains at different positions on the delay line are uncorrelated, which is the reason for the "US" in WSSUS.

The power spectrum of the complex gain fluctuations at a given tap delay ξ is proportional to the Fourier transform of $Q(\tau, \xi)$ with respect to τ. This power spectrum $S(\xi, \nu)$ has been called the "scattering function." It is given by

$$S(\xi, \nu) = \int Q(\tau, \xi) \exp(-j 2\pi\tau)\, d\tau. \tag{11}$$

The scattering function exhibits directly the delay and Doppler spreading characteristics of the channel.[2]

To make practical use of the WSSUS model, the functions $R(\Omega, \tau)$, $Q(\tau, \xi)$, and $S(\xi, \nu)$ must be regarded as mildly dependent on both time origin and carrier frequency as discussed in [1].

A cruder but frequently adequate description of the average fading dispersive properties of the WSSUS channel are provided by the delay and Doppler power spectra $Q(\xi), P(\nu)$ and their transforms, the frequency and time autocorrelation functions $q(\Omega), p(\tau)$, respectively. The latter are defined as

$$q(\Omega) = R(\Omega, 0) \tag{12}$$

$$p(\tau) = R(0, \tau). \tag{13}$$

$q(\Omega)$ is the complex cross-correlation coefficient between two received carriers as a function of their frequency separation.

When the frequency separation is such that the cross-correlation function $q(\Omega)$ is very near the maximum value $q(0)$ for all $|\Omega| < W_{coh}$ it is clear that all transmitted frequency components within a band of frequencies of width less than W_{coh} will be received fluctuating in a highly correlated fashion. For this reason W_{coh} is called the coherence bandwidth.

The time correlation function $p(\tau)$ is the autocorrelation function of the complex envelope of a received carrier. Clearly one may define a coherence duration parameter T_{coh} in terms of $p(\tau)$ in the same way as W_{coh} is defined in terms of $q(\Omega)$.

The gross channel parameters W_{coh} and T_{coh} are particularly

[2] $S(\xi, \nu)$ is also the two-dimensional power spectral density of the time variant transfer function, i.e., the double Fourier transform of $R(\Omega, \tau)$. $S(\xi, \nu)$ describes the intensity of scattering at a delay ξ and Doppler shift ν because of the correlation function relationship

$$\overline{U^*(\xi, \nu)U(\eta, \mu)} = S(\xi, \nu)\delta(\eta - \xi)\delta(\mu - \nu)$$

valid for the WSSUS channel.

useful in predicting the onset of frequency and time-selective distortion when the WSSUS channel contains no discrete paths. Then both $q(\Omega)$ and $p(\tau)$ drop to zero as $\Omega, \tau \to \infty$, and pulses with bandwidths greater than W_{coh} or time durations greater than T_{coh} will suffer ever increasing amounts of distortion. Contrast this situation with the mixed (specular-scatter) case (8), where $q(\Omega)$ and $p(\tau)$ approach nonzero constants as $\Omega, \tau \to \infty$. If the specular path is sufficiently strong, increasing the pulsewidth beyond T_{coh} or the bandwidth beyond W_{coh} may produce only a small amount of additional distortion. Of course if the specular component is very strong W_{coh}, T_{coh} may equal ∞ if they are defined as values of Ω and τ for which $q(\Omega)$ and $p(\tau)$ drop to a specific fraction of $q(0)$ and $p(0)$, respectively.

The Fourier transform of the frequency correlation function $q(\Omega)$ is the delay power spectrum $Q(\xi)$, which can be expressed in the following forms,

$$Q(\xi) = Q(0, \xi) = \int S(\xi, \nu)\, d\nu. \tag{14}$$

This function is proportional to the intensity of the complex tap gain at delay ξ in a differential tapped delay line model of the channel. One may define a multipath or delay spread parameter as the "width" of $Q(\xi)$ where width is defined in some convenient fashion.

Two measures of width that occur frequently in applications are "total" and "rms." The total delay spread L_{tot} is meant to define the extent of $Q(\xi)$ for values of ξ where $Q(\xi)$ is significantly different from zero [e.g., 40 dB down from the maximum value of $Q(\xi)$]. The utility of L_{tot} is that it defines the width of $g(t, \xi)$ versus ξ. Then, by Nyquist's sampling theorem, the transfer function $T(f, t)$ versus f must be sampled at least at a sampling "rate" of $1/L_{tot}$ samples/Hz to allow reconstruction of $T(f, t)$.

The rms delay spread L_{rms} is defined as twice the standard deviation of $Q(\xi)$ when it has been normalized to unit area and regarded as a probability distribution. This parameter may be shown to control the degree of frequency selectivity in a bandwidth that is of the order of the coherence bandwidth [1].

The Fourier transform of the time correlation function $p(\tau)$ is the Doppler power spectrum $P(\nu)$, which is the power spectrum of a received carrier. This spectrum may be expressed as an integration over $S(\xi, \nu)$:

$$P(\nu) = \int S(\xi, \nu)\, d\xi. \tag{15}$$

The "total" Doppler spread B_{tot} and rms Doppler spread B_{rms} parameters are defined analogous to L_{tot} and L_{rms}, respectively, and have analogous utilities.

When the product of the coherence bandwidth and time duration W_{coh}, T_{coh} of a channel exceeds the time-bandwidth product[3] of the signaling elements used in communicating over that channel, both time and frequency selective distortion will not be simultaneously active. Then $P(\nu)$ and $Q(\xi)$ [or equivalently $p(\tau)$, $q(\Omega)$] are sufficient to describe the average multipath and Doppler spreading characteristics of the channel. In effect, for the class of waveforms considered, one may replace the actual scattering function $S(\xi, \nu)$ by the simpler scattering function

$$S_0(\xi, \nu) = P(\nu)Q(\xi) \tag{16}$$

without altering the observed average time and frequency selective distortion on the received signals.

The reader should be reminded that to be practically meaningful, the functions $S(\xi, \nu)$, $P(\nu)$, $Q(\xi)$ must be regarded as slowly varying with time and generally dependent on carrier frequency, in addition to being dependent upon the physical location and motion of the terminals of the link.

C. Statistics

In order to be able to evaluate analytically the performance of various modulation techniques over a channel it is necessary to have more statistical information than the channel correlation functions defined in Section II-B. Strictly speaking, for an exact statistical characterization one needs multidimensional probability distributions of the system functions. Unfortunately, these have not been measured and if they were, they would be prohibitively complex to use. Fortunately, however, there are useful statistical models that may be used in characterizing radio links. All these models use Gaussian processes to model channel fluctuations either directly or indirectly. The utility of Gaussian characterization, either direct or indirect, is that the statistics can be completely specified from the correlation functions of the Gaussian processes.

Three very useful models that keep recurring are 1) the Gaussian WSSUS channel; 2) the Gaussian discrete WSSUS channel; and 3) the Gaussian phase-modulation discrete stationary channel.

The Gaussian WSSUS channel is a WSSUS channel in which the transmission of a carrier results in the reception of a narrow-band process whose in-phase and quadrature components are stationary Gaussian processes. A special case of this channel, which is the one most often used, is the complex Gaussian [2], [3] stationary scatter channel in which the in-phase and quadrature components of a received carrier are of equal strength and satisfy certain symmetry conditions that force the average

$$\overline{T(f, t)T(f + \Omega, t + \tau)} = 0. \tag{17}$$

Note that the left side of (17) is not the time-frequency correlation function because the conjugate sign is missing [c.f. (9)].

For the continuous portion of the line-of-sight (LOS) channel an examination [4] of the conditions leading to (17) reveals that whenever frequency selectivity is of significance for transmission bandwidths that are small compared to the carrier frequency (the usual situation) the correlation function in (17) is negligible compared to the time-frequency correlation function. The surface scatter channel generally contains both a diffuse channel component describable by a continuous $g(t, \xi)$

[3] Actually, one must use time-bandwidth "constraint" because coding techniques may open large time and frequency intervals.

and a discrete component (corresponding to reflection from the surface). It appears from the work of DeRosa [5] that the correlation function in (17) will also be negligible under the same conditions described for the LOS scatter channel. It may also be argued that under many conditions of interest the ionospheric scintillation and tropospheric refraction channels will satisfy (17).

One of the characteristics of the complex Gaussian channel is that a received carrier has an envelope that has the Rayleigh probability density function. Measurements of the distribution of received carrier envelopes for ionospheric reflection channels (HF channels) frequently exhibits the Rayleigh character and in modeling HF channels it has become customary to use the complex Gaussian model.

The utility of the complex Gaussian model is that the time-frequency correlation function $R(\Omega, \tau)$, or equivalently, $Q(\tau, \xi)$ or $S(\xi, \nu)$ completely specifies the statistics of the channel and frequently makes possible the analytic computation of error rates. In any case the Gaussian assumption allows the determination of system performance by hardware or software simulation techniques.

The Gaussian discrete WSSUS channel has the property that the fluctuations $G_k(t)$ in (6) have Gaussian (possibly nonzero mean) statistics. The complex Gaussian discrete WSSUS channel is of interest also, for which the moment property

$$\overline{(G_k - \overline{G_k})(G_j - \overline{G_j})} = 0 \tag{18}$$

applies.

The Gaussian phase-modulation discrete stationary channel is a stationary discrete channel in which $G_k(t)$ takes the form

$$G_k(t) = A_k \exp [j\phi_k(t)] \tag{19}$$

where A_k is constant and $\phi_k(t)$ is a Gaussian process. Note that in general $G_k(t)$ has a nonzero mean, i.e.,

$$\overline{G_k(t)} = A_k \exp (-\sigma_\phi^2/2), \tag{20}$$

where σ_ϕ is the rms value of the phase fluctuation.

In some applications σ_ϕ is so large compared to 2π that ϕ is regarded as uniformly distributed modulo 2π and $\overline{G_k} = 0$.

The stationary statistical models described above are convenient idealizations. However, the actual radio channel characteristics are nonstationary. Thus in the practical use of these models a quasi-stationary approach must be used with the channel correlation functions and others defining the statistics of the Gaussian processes, allowed to vary slowly with time, carrier frequency, and system geometry.

III. The Surface Scatter Channel

By the surface scatter channel we mean the collection of radio paths between a transmitter and receiver, which exist solely due to the intervention of the earth's surface, plus a distortion-free "direct path" between transmitter and receiver. The propagation effects on the direct path are not discussed in this paper. With regard to the present discussion, it is convenient to use the idealized direct path as a delay, Doppler, and amplitude reference for the indirect paths of the surface scatter channel.

A. Propagation Modeling

The basic areas of physics involved in modeling the propagation mechanisms of the surface scatter channel are the theories of scattering and reflection of radio waves from random surfaces separating media having different constitutive parameters. For aeronautical surface scatter channels the two media of interest are the air and the surface of the earth. Numerous papers have treated the problem of scattering from irregular surfaces. Beckmann and Spizzichino [6] summarize much of the work up to 1960.

When the surface is sufficiently smooth and flat it may be regarded as a plane interface between two media. The problem of determining the reflection from a plane lossy dielectric, while conceptually simple is quite involved because of the polarization and reflecting plane orientation angle dependencies. In the words of Stratton [14, p. 507], "... the complexity of what appeared to be the simplest of problems—the reflection of a plane wave from a plane absorbing surface—is truly amazing." The reader is referred to [14, sect. 9.4], [6, ch. 11], or [16, ch. 5] for a detailed discussion of this reflection problem. However it is appropriate to present here (Fig. 1) plots of the reflection coefficient magnitude and phase for the sea as a function of grazing angle γ (complement of angle between direction of propagation and normal to surface) for horizontal and vertical polarization at VHF ($\lambda = 230$ cm, $f_0 = 130$ MHz) and L band ($\lambda = 18.7$ cm, $f_0 = 1.6$ GHz).[4]

Note that horizontally polarized waves (no vertical component) are almost completely reflected, whereas vertically polarized waves (no component perpendicular to plane defined by direction of propagation and normal to surface) show a pronounced dip in reflection coefficient at low grazing angles. Also the phase of the reflection coefficient for horizontally polarized waves is essentially 180° while the phase for vertically polarized waves changes from 0° at large γ to 180° at low γ, reaching 90° at the grazing angle (called the Brewster angle) for which the magnitude of the reflection coefficient has a dip.

The plane sea reflection coefficients can be used for reflections off the sea except for small values of γ where the curvature of the earth must be taken into account. This is done by multiplying the reflection coefficient by a factor called the divergence coefficient (see [6, ch. 11] or [16, sect. 5.2]). For reflection off the earth between a synchronous satellite and an airplane at 10 and 20 km the divergence coefficient has dropped to only 0.95 and 0.90, respectively, at $\gamma = 10°$.

Scattering and reflection from land does not exhibit the statistical regularity as scattering and reflection from the sea. The reflection coefficients can have wide variations depending upon the electrical properties of the ground in the vicinity of the first few Fresnel zones. According to Spizzichino [6, p. 219] numerous investigators ([29] and others) have measured the reflection coefficients of different types of plane ground for various grazing angles. Plots of the magnitude and phase of the vertical and horizontal reflection coefficients for a surface with average conductivity and dielectric constant are

[4] From [15, p. 119, fig. 4.5].

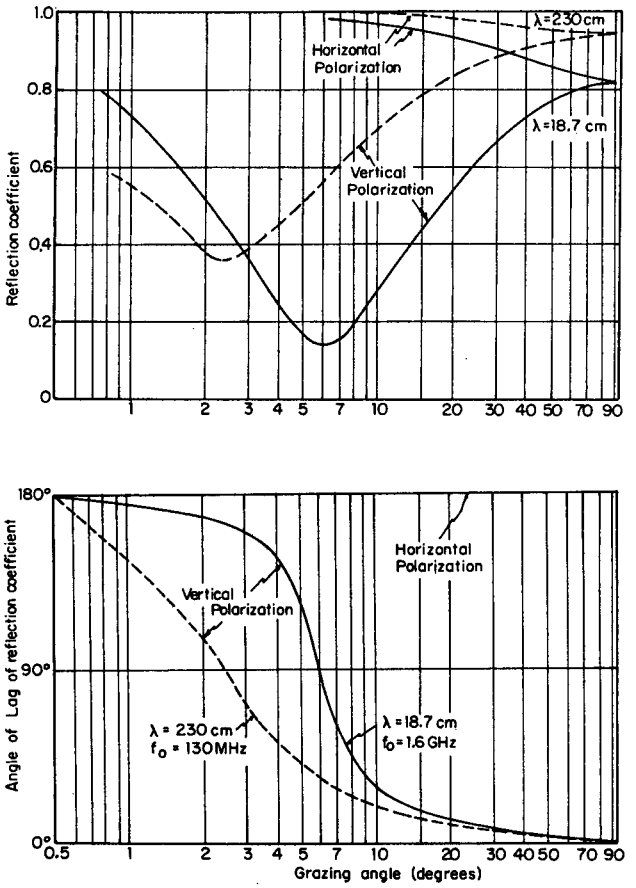

Fig. 1. Magnitude and angle of reflection coefficient Γ_0 of the smooth plane sea as a function of the grazing angle.

given in [6, figs. 11.1 and 11.3]. [30] presents graphs of reflection coefficients as a function of the conductivity and dielectric constant of the earth.

We turn now to a qualitative discussion of the return from the earth when the surface may not be considered smooth and flat. The analyses available generally assume a plane wave incident on the surface and characterize the signal scattered by the surface into different directions as measured very far from the surface. A reference direction that is singled out is the "specular" direction, defined as the direction that a reflected plane wave would take if the incident plane wave were reflected from a mirror located at the mean surface height.

To describe the character of the scattered signal it is necessary to define at least two statistical parameters of the surface: σ, the rms height fluctuation relative to the mean surface; and α, the rms value of the surface slope (spatial derivative of surface heights). It is assumed that the surface height fluctuations are member functions of a wide-sense-stationary two-dimensional random process. We consider the two limiting behaviors corresponding to $\sigma \to 0$ and $\alpha \to 0$.

When the surface height fluctuations are very small compared to a "surface" wavelength $\lambda/\sin\gamma$, where λ is the wavelength and γ the grazing angle, the surface behaves electrically like a smooth surface. In particular, all the energy is reflected in the specular direction and the received signal does not fluctuate if the surface is moved horizontally.[5] As σ increases, scattered signals appear in nonspecular directions. Moreover, as the surface is moved, the signals in the specular and nonspecular directions will fluctuate. It will be convenient to regard the scattered field as composed of two fields, one due to the average component and the other due to the fluctuating components. Assuming the scattering surface is very large in lateral extent, the average of the scattered signals are concentrated entirely in the specular direction. We call this field component the "discrete specular" component. The fluctuating, or as they are sometimes called, diffuse components may or may not be concentrated in the specular direction depending upon the value of the rms surface slope α. For very small values of α the diffuse scatter components will be concentrated in a narrow cone in the vicinity of the specular direction. Then it would be proper to lump the diffuse scatter components together and call them the "diffuse specular component."

The statistical character of the signal fluctuations observed in the specular direction can have several forms. If the spatial correlation length of surface height fluctuations L (of the order of σ/α) is much larger than the dimensions of the first Fresnel zone,[6] a carrier received in the specular direction will be phase modulated (by a horizontally moving surface) with a phase $4\pi h/\lambda \sin\gamma$, where h is the surface height at the first Fresnel zone relative to mean surface ($\sigma^2 = \overline{|h|^2}$). Thus the statistics of the phase modulation will be the same as those of the surface height fluctuation. For a mean squared modulation index $(4\pi)^2(\sigma/\lambda)^2 \sin^2\gamma \gg 1$ there will be no steady carrier component in the received carrier. If the spatial correlation length L is much smaller than the dimensions of the first Fresnel zone, the signal received in the specular direction will be the sum of many independent fluctuating components. From the central limit theorem one argues that the in-phase and quadrature components of the received carrier will be normally distributed. For $(4\pi)^2(\sigma/\lambda)^2 \sin^2\gamma \gg 1$, the steady carrier component vanishes and the complex envelope of the fluctuating carrier may be characterized as a complex Gaussian process. In the nonspecular directions the situation is simpler. No steady components exist, and, assuming the dimensions of the reflecting surface to be very large compared with the correlation length L, the received fluctuating carrier can be characterized approximately as a complex Gaussian process.

We consider now some formulas that have been derived for specular and diffuse scattering for a surface with Gaussian

[5] Instead of considering the effect of moving the surface one may observe the effect of representing the surface by different member functions of the ensemble defining the surface height statistics.

[6] The nth Fresnel zone is a region on the surface for which the path delay between transmitter and receiver differs from that of the specular path delay by an amount between $n(T/2)$ and $(n-1)(T/2)$ where T is the duration of an RF cycle. The quoted conditions leading to phase modulation can only be readily proved when $\gamma = 90°$ where the Fresnel zones become the region between concentric circles, because only in this case has it been proved that most of the energy reflected from a flat surface comes from the first few Fresnel zones. However one may reason heuristically that the same result will apply if γ does not become too small.

height statistics. In the case of a sea surface, at least, Cox and Munk [7] have found the Gaussian approximation to be quite good.

The most widely used method for analyzing the electromagnetic signals scattered from a lossy dielectric, such as the earth and sea, is based upon an approximation that is sometimes called the "Kirchhoff approximation" [6]. This approximation involves the assumption that the fields existing at a point on the surface are identical to those that would exist on a plane tangent to the surface at that point. According to Brekhovskikh [8] this approximation is valid if the wavelength of the radiation divided by $4\pi \sin \gamma$ is much smaller than the local radius of curvature of the surface.

Another method that has been used more recently and that we shall discuss briefly is called the "method of small perturbation." This method applies to the case of irregularities that are small compared to a wavelength. In either case diffuse scattering is handled from an engineering point of view by calculating equivalent radar cross sections per unit area of surface. The received diffuse signal is determined by summing the returns from elemental areas with each area defined by a suitable scattering cross section.

The discrete specular component is characterized by a reflection coefficient that differs from that of a smooth surface by a factor that accounts for the roughness of the surface. In [6] it is shown that for Gaussian height statistics the reflection coefficient is given by

$$\Gamma = \Gamma_0 D \exp\left(-\tfrac{1}{2}\left[4\pi(\sigma/\lambda)\sin\gamma\right]^2\right) \tag{21}$$

where γ is the grazing angle for specular reflection, Γ_0 the reflection coefficient for a plane surface of the same material, and D the divergence coefficient. [6, ch. 14] discusses measurements that have been made of Γ for different surfaces and compares these results with (21), (see [6, p. 318, fig. 14.1]). According to the author, general agreement with (21) may be seen in the experimental results.

Using the Kirchhoff approximation, plus additional simplifying assumptions, several authors [9]-[13] and [16] have computed scattering cross section per unit area. A number of different scattering cross sections may be defined. Thus one may define four scattering cross sections σ_{HH}, σ_{HV}, σ_{VH}, and σ_{VV} according to whether horizontal or vertical polarization is transmitted and whether the receiving antenna is polarized horizontally or vertically. Or one may define scattering cross sections that include the total power scattered into both polarizations for a transmitted signal with horizontal or vertical polarization.

Stogryn [10] has calculated σ_{HH}, σ_{HV}, σ_{VH}, and σ_{VV} for a rough lossy dielectric Gaussian distributed surface assuming in addition to the Kirchhoff approximation that the electrical roughness parameter

$$g = (2\pi\sigma/\lambda)(\sin\gamma + \sin\theta) \tag{22}$$

is much greater than unity. As shown in Fig. 2, θ is an angle analogous to the grazing angle γ for a scattered wave. Virtually all results of any simplicity by the various authors assume $g \gg 1$.

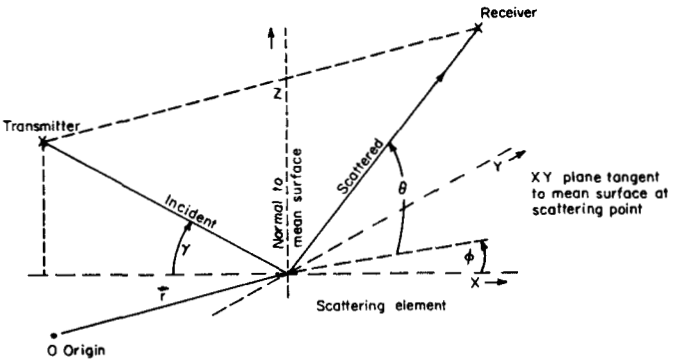

Fig. 2. Definition of angles in scattering.

The simplest result available on scattering cross section using the Kirchhoff approximation is presented in Beckmann and Spizzichino (see [6, p. 89, eq. (63) and p. 251, eq. (7)]).[7] We present this result in a more general form regarding dependence on the spatial correlation function of wave heights. To wit, the scattering cross section/unit area at the point on the surface having the radius vector coordinate r from some origin[8] is given by

$$\sigma(r) = \frac{1}{2\alpha^2 \cos^4\beta} \exp\left(-\frac{\tan^2\beta}{2\alpha^2}\right), \quad g^2 \gg 1, \tag{23}$$

where β is a complicated function of γ, θ, and ϕ (see Fig. 2) that has the simple physical interpretation of being the tilt angle of a plane at r relative to a tangent plane to the mean surface at r required for mirror reflection from transmitter to receiver. The parameter α is the rms value of the spatial derivative of surface heights. In [6] a spatial correlation function of the form

$$C(l) = \exp\left(-l^2/L^2\right) \tag{24}$$

was used in deriving (23), where L may be viewed as a spatial correlation distance of height fluctuation. When the spatial correlation function assumes the particular form (24) one may readily show that

$$\alpha = \sqrt{2}\,\sigma/L. \tag{25}$$

However, (23) shows that for $g^2 \gg 1$, the scattering cross section does not depend upon the shape of the spatial correlation function but only on a single parameter α, the rms value of surface height derivatives. The most extensive experimental investigation of sea surface slopes may be found in the work by Cox and Munk [7]. From their results one may estimate

[7] We have normalized to present the radar cross section per unit area as defined in this paper.

[8] Although the derivation in [6] assumes a flat mean surface the results for scattering cross section should be independent of the shape of the mean surface provided that the curvature of the mean surface is very small over a region whose dimensions are of the order of the spatial correlation of wave-height fluctuations about the mean surface. This does appear to be the usual case, so we shall quote results for scattering cross section in this more general form.

values for the parameter α. Thus at a wind speed of 20 knots one may estimate $\alpha = 0.12$ and for a wind speed of 10 knots $\alpha = 0.10$.

The scattering cross section (23) was calculated under the assumption of a perfectly conducting surface and included the combined power in the horizontal and vertical polarizations, assuming either horizontal or vertical polarization was transmitted. It does not include certain effects that take place at small grazing angles, such as wave shadowing effects and multiple scattering. Beckmann [6, p. 98] suggests that $\sigma(r)$ can be corrected for a lossy dielectric surface through multiplication by an averaged squared Fresnel reflection coefficient. However Stogryn [10, eqs. (61a) and (61b)] has made the more exact calculations (again for $g >> 1$) and they do not agree with Beckmann's suggestion because of the existence of cross-polarized terms. For small cross-polarized power (which appears to be valid for the sea scatter), Beckmann's suggestion is reasonable.

Following this suggestion, one would use $\sigma_f(r)$, instead of $\sigma(r)$,

$$\sigma_f(r) = |\Gamma_0|^2 \sigma(r), \tag{26}$$

where Γ_0 is the Fresnel reflection coefficient corresponding to reflection from a plane lossy dielectric surface oriented for mirror reflection from transmitter to receiver at the surface location r. [6, ch. 15] discusses the results of experimental investigations of diffuse scattering from the earth's surface. The work of Bullington [31], Beard *et al.* [32], and MacGavin and Maloney [33] is discussed in detail. The measured $\sigma(r)$ are always widely scattered "about a mean value which varies between 0.30 and 0.35. The majority of the values are included between 0.2 and 0.4." It was also found that the results were approximately independent of grazing angle and wavelength as is predicted for (23).

Returning now to (23) we note that $\sigma(r)$ decreases rapidly for r locations requiring $\tan\beta$ to be any significant amount bigger than α. (At $\tan\beta = 2\alpha$, $\sigma(r)$ has decreased to 13 percent of the value at $\beta = 0$.) The region of the surface for which $\sigma(r)$ is of significant value relative to its value at $\beta = 0$ has been called the "glistening" region because it defines the surface element locations actively participating in the diffuse scattering process.

To explain the possible restrictive nature of $g^2 >> 1$, we have used Kerr's table [16, p. 489] for the first 3 columns of Table I, which show the relationship between the seaman's "sea state" and approximate ranges of crest to trough wave heights Δh. The fourth and fifth columns present $4\pi\sigma/\lambda$ for 150 MHz and 1.5 GHz, where we have assumed that the peak-to-peak fluctuations of the sea (taken as Δh) are equal to 4 times the standard deviation σ (with this assumption the probability of the sea-surface height Gaussian process exceeding Δh is approximately 4 percent).

The roughness parameter g may be expressed in the form

$$g = (4\pi\sigma/\lambda) \sin\bar{\gamma} \tag{27}$$

where the angle $\bar{\gamma}$ is defined implicitly by

$$\sin\bar{\gamma} = \tfrac{1}{2}(\sin\gamma + \sin\theta). \tag{28}$$

The values of γ, θ of interest are associated with those points on the surface within the glistening region. The point of mirror reflection between transmitter and receiver for the mean surface, called the specular point, corresponds to $\beta = 0$ and $\gamma = \theta = \bar{\gamma} = \gamma_{sp}$. As the scattering point departs from the specular location γ and θ will generally differ. We have defined $\bar{\gamma}$ as a convenient single-angle approximation to the average value of γ, θ, which is exact for small γ, θ. Columns 6 and 7 in Table I present the values of $\bar{\gamma}$ required to make the roughness parameter $g = 1$ for the various sea states. For g to any extent greater than unity, say 3 or greater, one may assume the condition $g^2 >> 1$ satisfied. Also, if $\bar{\gamma}$ does not differ too much from γ_{sp}, we see that $g^2 >> 1$ implies negligible discrete specular component and $g = 1$ implies that the discrete specular component has decreased to e^{-1} of its value for a calm sea. We note from Table I that except for very small grazing angles, $g^2 >> 1$ is a reasonable assumption for 1.5 GHz. However, for 150 MHz this assumption will be violated for many grazing angles of interest. Thus care must be taken in applying (23) at VHF frequencies.

From results given in [6, p. 79, eq. (31)] one may show that the scattering cross section given by the following integral does not require $g^2 >> 1$

$$\sigma(\bar{r}) = \frac{1}{\cos^4\beta} \int_0^\infty l J_0(l\tan\beta) \left\{ \exp\left[-g^2 \left(1 - C\left(\frac{\sigma}{g} l\right)\right]\right] - \exp\left[-g^2\right] \right\} dl \tag{29}$$

where $J_0(\cdot)$ is the Bessel function of zeroth order and $C(\cdot)$ the assumed isotropic spatial correlation function of wave heights [e.g., see (24)]. Equation (29) is based upon the Kirchhoff approximation (surface radius of curvature large compared to $\lambda/4\pi \sin\gamma$), perfectly conducting surface, and no shadowing or multiple scattering. Since the Kirchhoff approximation itself must break down at low grazing angles and shadowing is neglected, (29) must become invalid at sufficiently low grazing angles.

The other technique of surface scatter modeling, frequently called the "small perturbation method," accounts for scattering from irregularities small compared to a wavelength. This method has been found particularly effective in explaining the results of radar backscatter measurement at low grazing angles [17], where the scatter cross section predicted by the Kirchhoff method drops to zero very rapidly. The earliest work on the small perturbation method was carried out by Rice [18]. Some years later two schools of investigation developed, one in the U.S. (e.g., [19], [20]) based upon the work of Rice, and one in the Soviet Union (e.g., [21], [22]). Presently a "two-scale" or "composite" model is used to characterize radar backscatter, combining the results of the Kirchhoff and small perturbation methods. A detailed chronology of the development of the large-scale Kirchhoff and composite models and a detailed mathematical development of the latter model is given by DeRosa [23].

Surface scatter channel modeling for the aeronautical channel involves a forward scatter mechanism. For this case, in

TABLE I
RELATIONS BETWEEN ELECTRICAL ROUGHNESS AND SEA ROUGHNESS

No.	Sea State	Wave Height Δh	$\frac{4\pi\sigma}{\lambda} = \frac{g}{\sin \bar{\gamma}}$		$\bar{\gamma}$, in Degrees, for g = 1	
			150 MHz	1.5 GHz	150 MHz	1.5 GHz
0	Calm	0	0	0	-	-
1	Smooth	0 - 1 ft	0 - .47	0 - 4.7	-	> 12.3
2	Slight	1 ft - 3 ft	.47 - 1.41	4.7 - 14.1	> 45	12.3 - 4.1
3	Moderate	3 ft - 5 ft	1.41 - 2.35	14.1 - 23.5	45 - 25	4.1 - 2.4
4	Rough	5 ft - 8 ft	2.35 - 3.77	23.5 - 37.7	25 - 15.4	2.4 - 1.5
5	Very Rough	8 ft - 12 ft	3.77 - 5.64	37.7 - 56.4	15.4 - 10.2	1.5 - 1.0
6	High	12 ft - 20 ft	5.64 - 9.40	56.4 - 94	10.2 - 6.1	1.0 - .6
7	Very High	> 20 ft	> 9.40	> 94	< 6.1°	< .6

contrast to backscatter, the power does not drop off rapidly at low grazing angles and, moreover, a strong specular component may appear. A quantitative comparison of scatter cross sections/unit area may be made for the Kirchhoff and small perturbation methods in forward scatter, but the author is not aware of such a comparison. We present such a comparison for one case, horizontal polarization and a perfectly conducting surface.

The small-scale surface height fluctuations will be modeled as Gaussian with (isotropic) spatial correlation function

$$C(l) = \sigma_1^2 \exp\left[-(l^2/L_1^2)\right] \tag{30}$$

where σ_1 is the rms value of the surface height fluctuation and L_1 the correlation distance. In order for the small perturbation method to be applied, certain inequalities must be valid [22, pt. II, p. 561].

$$\frac{2\pi|\xi|}{\lambda} \ll 1 \qquad \left|\frac{d\xi}{ds}\right|^2 \ll 1 \tag{31}$$

where ξ is the surface height deviation from the mean surface and $d\xi/ds$ is the height spatial derivative. If we replace $|\xi|$ and $|d\xi/ds|^2$ in (31) by their averages, these inequalities become

$$\sigma_1 2\sqrt{2\pi}/\lambda \ll 1 \qquad 2(\sigma_1/L_1)^2 \ll 1. \tag{32}$$

Using the surface model defined above, the small perturbation method (SPM) shows that the scattering cross section per unit area for horizontal polarization and a perfectly conducting surface (see Swift [23, eq. (14)] with plus sign corrected to minus sign or DeRosa [5, p. 113, eq. (43)] can be placed in the form

$$[\sigma(\boldsymbol{r})]_{\text{SPM}} = 2\pi^3 \left(\frac{\sigma_1 2\sqrt{2\pi}}{\lambda}\right)^4 \left(\frac{L_1}{\sigma_1}\right)^2 \sin^2\gamma \sin^2\theta \cos^2\phi \cdot \exp\left(-\frac{L_1^2}{\sigma_1^2}\left(\frac{2\pi\sigma_1}{\lambda_1}\right)^2 \left(\frac{\sin\gamma + \sin\theta}{2}\right)^2 \tan^2\beta\right). \tag{33}$$

A study of (33) with careful attention to the inequalities (32) does not indicate a well-defined localized glistening region for small values of β as for the Kirchhoff model's scattering cross section (24). Taking the ratio of the two scattering cross sections at the specular point ($\beta = 0, \gamma = \theta, \phi = 0°$) yields

$$\left.\frac{[\sigma(\boldsymbol{r})]_{\text{SPM}}}{[\sigma(\boldsymbol{r})]_{\text{KM}}}\right|_{\substack{\text{specular}\\ \text{point}}} = (2\pi)^3 \left(\frac{\sigma/L}{\sigma_1/L_1}\right)^2 \left(\frac{2\sqrt{2\pi}\,\sigma_1}{\lambda_1}\sin\gamma\right)^4. \tag{34}$$

If one may assume the slopes of the small scale ripples modeled by SPM are comparable to those of the large scale "swells" modeled by the Kirchhoff method (KM) it becomes evident that in the glistening region of the large-scale swells, at least the scattered power of the small-scale ripples is likely to be small compared to that due to the large-scale swells. This indicates that the small-scale scatter may not be important for forward scatter channels over the ocean.

B. System Function Modeling

The previous section has summarized some important radio propagation aspects of surface scatter channel modeling. Here we wish to relate these propagation considerations to the "blackbox" or system function modeling of the surface scatter channel, which is of direct importance in modem design.

For the purposes of such modeling, the surface scatter channel may be thought of as the parallel combination of three subchannels, a direct path channel, a discrete specular reflection channel, and a diffuse scatter channel. Thus the complex envelope of the received signal may be expressed as the sum

$$w(t) = w_{\text{dir}}(t) + w_{\text{sp}}(t) + w_{\text{dif}}(t) + \eta(t), \tag{35}$$

where $\eta(t)$ is an additive noise term and the subscripts identify the other terms as contributions from the three subchannels in Fig. 3.

1) Direct Path Channel: As discussed previously, in the case of the surface scatter channel as defined in this paper, we do not include tropospheric and ionospheric channel effects. Thus propagation through the atmosphere between two points is characterized for the surface scatter channel simply by means of a (time varying) delay, complex gains associated with antenna patterns, and free-space losses. In particular the received signal from the direct path channel is given by

$$w_{\text{dir}}(t) = G_{\text{dir}} z(t - \tau_{\text{dir}}) \exp\left[-j 2\pi f_0 \tau_{\text{dir}}(t)\right], \tag{36}$$

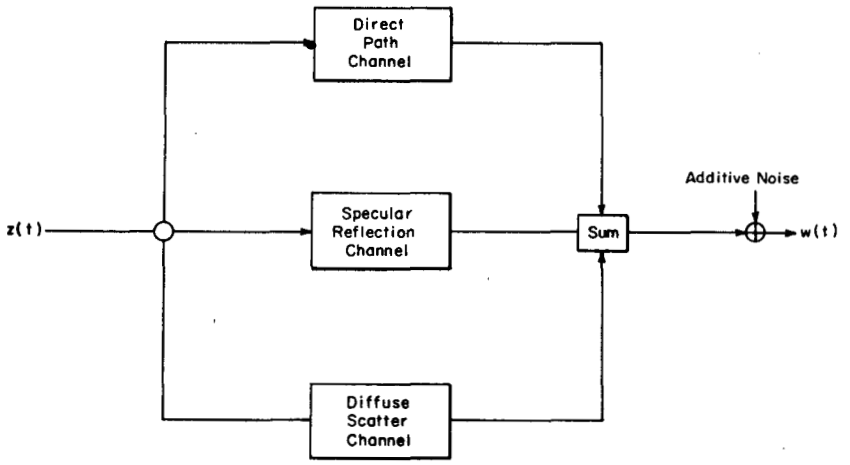

Fig. 3. Representation of surface scatter channel.

where G_{dir} is a slowly varying complex gain due to transmitter and receiver antenna patterns and free-space losses, f_0 the carrier frequency, and $\tau_{dir}(t)$ the line-of-sight path delay. As far as the modulation $z(t - \tau_{dir})$ is concerned, $\tau_{dir}(t)$ is a slowly varying delay that must be adequately tracked for synchronization in data reception or measured in the case of ranging systems. As far as the exponential term in (36) (due to the delayed carrier) is concerned, however, $\tau_{dir}(t)$ produces a rapidly time variant phase shift $2\pi f_0 \tau_{dir}(t)$ and a slowly varying Doppler shift ν_{dir},

$$\nu_{dir} = f_0 \frac{d\tau_{dir}(t)}{dt} = \frac{f_0}{c} V_{dir}, \tag{37}$$

where c is the velocity of light and V_{dir} the rate of change of the path length from transmitter to receiver. Expressions for G_{dir} and τ_{dir} are readily obtained from the geometry, velocity vectors, and antenna characteristics of the transmitter and receiver and will not be presented here.

2) Specular Reflection Channel: The specular reflection channel is used to characterize $w_{sp}(t)$ the received signal due to the average (over the surface heights) field discussed in Section III-A. Assuming a very large scattering surface, this field is focused entirely in the specular direction and behaves, apart from a complex gain, similar to a mirror reflection from the surface. Thus

$$w_{sp}(t) = \Gamma G_{sp} z(t - \tau_{sp}) \exp [-j 2\pi f_0 \tau_{sp}(t)] \tag{38}$$

where Γ is a complex gain (given by (21) by Kirchhoff model surface) that accounts for the electrical and roughness properties of the surface, G_{sp} a slowly varying complex gain due to complex antenna gains of the transmitter and receiver in the specular direction and free-space path losses, and $\tau_{sp}(t)$ the total path delay from transmitter to specular reflection point to receiver. From a mathematical point of view $w_{sp}(t)$ has the same structure as $w_{dir}(t)$, (36). The difference lies in the relative complex gains, delays, and Doppler shifts. A detailed set of delays and Doppler shifts for the direct path and specular channels is given in [15] for an airplane to synchronous satellite link.

A useful approximate expression for the time-delay difference between the specular reflection and direct path channels for the case of an airplane to synchronous satellite link (accurate down to $\gamma = 15°$ according to [15]) is given by

$$\tau_{sp} - \tau_{dir} = (2H/c) \sin \gamma \tag{39}$$

where H is the height of the aircraft. For an aircraft at 20 km and 20° grazing angle this time-delay difference is 45 μs.

The Doppler shift difference

$$\nu_{sp} - \nu_{dir} = f_0 \frac{d}{dt} (\tau_{sp} - \tau_{dir})$$

$$= \frac{f_0}{c} (V_{sp} - V_{dir}), \tag{40}$$

where V_{sp} is the rate of change of the transmitter-specular point-receiver path distance, and ν_{sp} the Doppler shift on the specular reflection channel. The Doppler shift difference is usually quite small. We quote some results from [15] for the airplane-satellite channel. For horizontal flight in the great circle plane containing specular point, airplane, and satellite, the maximum Doppler shift has a broad maximum between 10° and 30° for airplane heights of 10–20 km and airplane velocities of 600–1600 knots. For 1600 knots and 20 km the Doppler shift difference is 5 Hz. Motion at right angles to the great circle plane produces no Doppler shift. Vertical motion of the aircraft will produce a Doppler shift difference. At L band (1.6 GHz) and 20-degree grazing angle this Doppler difference is around 3.5 V Hz where V is the vertical velocity in meters/second.

The importance of the specular component depends on the size of the reflection coefficient Γ and antenna discrimination against energy from the specular direction. Over the North Atlantic it appears that at L band the surface is rough enough to make the specular reflection channel negligible most of the time. However, at VHF the specular reflection channel can produce a significant output relative to the direct path. As discussed in Section III-A, the simple surface scattering model provided by the Kirchhoff approximation will be valid much less in-land than over the sea. At any rate, as the terrain changes in the vicinity of the Fresnel zone, one may expect

that $|\Gamma|$ will vary from negligible values to values close to unity (over a lake perhaps).

3) Diffuse Scatter Channel: The diffuse scatter channel accounts for all received signals other than those due to the direct path and the discrete specular path. Over the ocean the diffuse scatter paths produce a continuum of infinitesimal contributions to the received signal, and the diffuse channel is generally representable as a random time-varying dispersive filter with a time variant impulse response containing no discrete components. (The only exception is in the limiting case of very small rms slope α, when the diffuse paths concentrate so closely in the specular direction that the entire diffuse scatter channel may be approximated by a single fluctuating discrete path having the same path delay as the discrete specular component.)[9] In addition, enough statistical regularity exists in the surface fluctuations so that quasi-stationary WSSUS models with associated channel correlation functions (e.g., frequency correlation function, Doppler power spectra, delay-Doppler scatter functions) represent useful means of characterization. Moreover, with the aid of the Kirchhoff and small perturbation methods, one may obtain meaningful estimates of channel correlation functions for some cases of interest.

Over land, the characterization problem is considerably more difficult. The scattering surface exhibits far greater statistical irregularity (desert, foliage, mountains, cities, etc.) and the Kirchhoff and small perturbation methods will only be useful for a fraction of the scattering surfaces. While a continuum of return paths is likely, there will be situations where strong localized reflections may occur, such as reflections from man-made metallic structures (e.g., buildings) and natural objects (e.g., mountains). When such localized reflections occur, one must add discrete multipath components to the diffuse channel as defined here. It is still likely that a quasi-stationary WSSUS channel is useful. However, much more rapid changes in the channel correlation functions are to be expected. In any case the received signal due to the diffuse scatter channel can be represented by

$$w_{\text{dif}}(t) = \int z(t-\xi)g(t,\xi)d\xi, \tag{41}$$

where $g(t, \xi)$ is the impulse response of the diffuse scatter channel.

In this subsection we discuss the evaluation of channel correlation functions for the diffuse scatter channel assuming the Kirchhoff model and present some theoretical results for an airplane-synchronous satellite channel.

Two general approaches have been used to determine system function characteristics for the surface scatter link. One approach makes use of normalized scattering cross sections, such as those discussed in Section III-A, to directly formulate integral expressions for channel correlation functions (e.g., frequency correlation function $q(\Omega)$, Doppler power spectrum $P(\nu)$, scattering function $S(\xi, \nu)$). This approach has been used by Mallinckrodt [24], [28], Staras [25], Durrani and Staras [26], and DeRosa [27]. It is implicit in such calculations that the channel may be characterized as a WSSUS channel. The other approach is more basic, starting with the formulation of expressions (usually integrals) for system functions (e.g., time-variant transfer functions) and then proceeding to the averaging required to determine channel correlation functions. The latter approach provides the means for answering basic questions not obtainable by the scattering cross-section formulation, such as the degree of statistical dependence between signals received on different polarizations and the validity of the quasi-WSSUS channel model. The more basic formulation has been carried out by DeRosa [5] for a composite surface consisting of the combination of large-scale fluctuations (satisfying the requirements of the Kirchhoff method) and small-scale fluctuations (satisfying the requirements of the small perturbation method).

We first present the simplest nontrivial results derived from the use of scattering cross sections. These involve the computation of the frequency correlation function $q(\Omega)$, delay power spectra $Q(\xi)$, Doppler power spectrum $P(\nu)$, time correlation function $p(\tau)$, time–frequency correlation function $R(\Omega, \tau)$, scatter function $S(\xi, \nu)$, and cross-power spectral density function $P(\Omega, \nu)$. Approximate expressions for these functions will be derived for the channel between an aircraft and a synchronous satellite. The results presented here are derived under the same conditions and with the same "steepest descent" approximations as those of Mallinckrodt [24], [28] who derives expressions for $Q(\xi), P(\nu), S(\xi, \nu)$ and Staras [25] who derives expressions for $q(\Omega)$ and $p(\tau)$. The results of these authors are compared and generalized to include an arbitrary direction of the airplane velocity vector and analytic expressions for $R(\Omega, \tau)$ and $P(\Omega, \nu)$.

The earth is assumed to have a flat mean surface with Gaussian-distributed surface heights relative to the mean and sufficiently smooth fluctuations to satisfy the requirements of the Kirchhoff method. In addition the roughness criterion

$$g^2 = [(2\pi\sigma/\lambda)(\sin\gamma + \sin\theta)]^2 >> 1 \tag{42}$$

is assumed to apply over the glistening region so that the simple expression (23) for normalized scattering cross section may be used. Finally it is also assumed that the rms surface slope $\alpha << 1$ and the deviation angle $\theta >> \alpha$. Even with all these assumptions, it appears that these results should provide useful channel information for some L-band oceanic airplane-to-satellite channel over the North Atlantic. It should be realized, however, that the case $\theta >> \alpha$ will be violated under some conditions of interest in aeronautical communications (in particular, sufficiently low elevation angles or rough surfaces).

For easy reference we repeat the expression (23) for the scattering cross section per unit area (including the approximation (26) for a nonperfect conducting surface),

$$\sigma(r) = |\Gamma_0|^2 \frac{1}{2\alpha^2 \cos^4\beta} \exp\left(-\frac{\tan^2\beta}{2\alpha^2}\right), \quad g^2 >> 1, \tag{43}$$

[9] This diffuse contribution previously was called a "diffuse specular component."

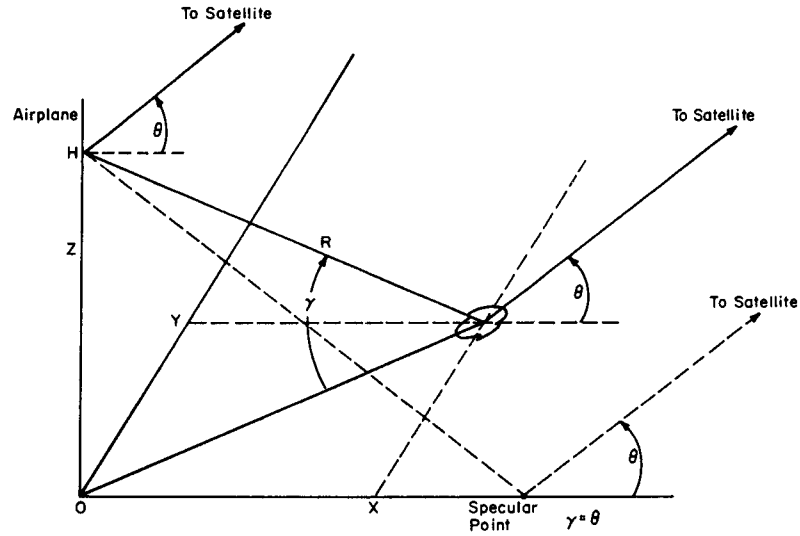

Fig. 4. Geometrical relationships for scattering in airplane-synchronous satellite channel assuming flat mean earth surface.

where Γ_0 is the appropriate Fresnel reflection coefficient (horizontal or vertical) for a flat ocean, α the rms sea slope, and β the tilt angle of a plane at r relative to a tangent plane to the mean surface at r required for mirror reflection from transmitter to receiver.

For a flat mean surface and a satellite very far from the airplane, Fig. 4 depicts geometrical relationships for the scattering process. As the origin of the coordinate system we have chosen the point on the mean surface directly below the aircraft, so that the airplane coordinates are $(0, 0, H)$ where H is the height of the aircraft. The satellite is assumed to be in the XZ plane, so far from the airplane and scattering surface that rays leaving the airplane and any scattering points on the glistening zone and terminating on the satellite have essentially the same elevation angle θ, as shown in Fig. 4. At the specular point, located on the X axis, the grazing angle $\gamma = \gamma_{sp} = \theta$.

Due to our assumed coordinate system we may express $\sigma(r)$ as a function of the rectangular surface coordinates X, Y, i.e., $\sigma(r) = \sigma(X, Y)$. The incremental power transferred from transmitter to receiver normalized to the power received on the direct path for a small area $\Delta x \Delta y$ is given by

$$\frac{\Delta P_S}{P_D} = |\Gamma_0|^2 \frac{\sigma(X, Y) R_0^2}{4\pi R^2 R_2^2} A(X, Y)\, \Delta x \Delta y$$

$$\approx |\Gamma_0|^2 \frac{\sigma(X, Y)}{4\pi R^2} A(X, Y)\, \Delta x \Delta y, \qquad R_0 \approx R_2, \tag{44}$$

where R_0, R, R_2 are the lengths of the direct path, the path from airplane to scattering area element, and the path from scatterer to satellite, respectively; $A(X, Y)$ is the surface illumination pattern of the combined transmitter and receiver antenna gains normalized to the direct path gains; and P_S, P_D are the total scattered and direct path powers. The total normalized scattered power is then

$$\frac{P_S}{P_D} = |\Gamma_0|^2 \iint_{-\infty}^{\infty} W(X, Y) A(X, Y)\, dx\, dy, \tag{45}$$

where

$$W(X, Y) = \frac{\sigma(X, Y)}{4\pi(X^2 + Y^2 + H^2)}. \tag{46}$$

For small α, $\sigma(X, Y)$ and $W(X, Y)$ will be concentrated in the vicinity of the specular point $(H/\tan\theta, 0, 0)$ and will decrease to negligible values rapidly outside the glistening zone. The steepest descent approximations used in Mallinckrodt [24], [28] and Staras [25] and also in the simple derivations to be given here, represent the argument of the exponent in $W(X, Y)$ by the leading nonvanishing terms in a Taylor series expansion of the surface coordinates about the specular point (Mallinckrodt used rectangular coordinates and Staras used polar coordinates). Any expressions multiplying the exponential terms are represented by their value at the specular point. This approximation should be useful when $\theta >> \alpha$.[10] With this approximation

$$W(X, Y) = W(X) W(Y) = \frac{1}{2\alpha H \csc^2\theta \sqrt{2\pi}}$$

$$\cdot \exp\left(-\frac{(X - H \operatorname{ctn}\theta)^2}{8\alpha^2 H^2 \csc^4\theta}\right) \frac{1}{2\alpha H\sqrt{2\pi}} \exp\left(-\frac{Y^2}{8\alpha^2 H^2}\right), \tag{47}$$

[10] It is readily shown that in the plane $Y = 0$, $\beta = (\theta - \gamma)/2$. Thus when $\beta = \theta/2$, there can be energy scattered to the receiver by areas at infinity on a plane surface. Of course on a spherical earth $\gamma = 0$ corresponds to the points at which planes through the airplane are tangent to the earth. In the former case the glistening zone extends to infinity and in the latter case it is still so large as to violate the conditions required for the use of (44). If $\alpha << \theta$ one may argue that the power returned at values of β that violate (44) will be negligible. However the author is not aware of any critical analysis to determine simple criteria for use of (44).

which may be recognized as the product of the probability density function of two normally distributed random variables, the X variable having mean H ctn θ and standard deviation $2\alpha H \csc^2 \theta$ and the Y variable having zero mean and standard deviation $2\alpha H$. Use of (47) in (45) shows that when the surface illumination pattern varies little over the glistening region

$$P_S/P_D \approx |\Gamma_0|^2 A(H/\tan\theta, 0). \tag{48}$$

We consider now the case wherein (48) applies and determine expressions for channel correlation functions. To determine the Doppler power spectrum $P(\nu)$, delay power spectra $Q(\xi)$, or delay-Doppler scatter function $S(\xi, \nu)$, one may associate a single delay and Doppler shift and a particular power density with each differential area of the surface.[11] By expressing the Doppler shift ν as a function of X and Y, and regarding X, Y as random variables, the probability density function of ν will be identical to the desired Doppler power spectrum, normalized to unit area. The factor $|\Gamma_0|^2 A(H/\tan\theta, 0)$ may then be applied to correct the height of $P(\nu)$. An exactly analogous procedure will be used to derive $Q(\xi)$ and $S(\xi, \nu)$ as probability density functions of the random variable ξ and the joint variable (ξ, ν). The Fourier transforms of $P(\nu)$, $Q(\xi)$, $S(\xi, \nu)$, $p(\tau)$, $q(\Omega)$, and $R(\Omega, \tau)$, respectively, may be regarded as characteristic functions of the variables ν, ξ, (ν, ξ).

If V is the velocity vector of the airplane, it is seen that the Doppler shift associated with the received signal from a scattering element is given by

$$\frac{f_0}{c} V \cdot \left(\frac{R}{R}\right) = \frac{f_0}{c}\left(V_x \frac{X}{R} + V_y \frac{Y}{R} - V_z \frac{H}{R}\right), \tag{49}$$

where R is a vector extending from the airplane to the scattering element. The Doppler shift relative to that produced by an element at the specular point is

$$\nu = \frac{f_0}{c} V_x \left(\frac{X}{R} - \cos\right) + \frac{f_0}{c} V_y \frac{Y}{R} + \frac{f_0}{c} V_z \left(\sin - \frac{H}{R}\right). \tag{50}$$

Following the procedure described above, ν is to be regarded as a random variable related to the random variables X and Y by (50). The probability density function of ν is the normalized Doppler power spectrum. Before determining the density function of ν we approximate ν by leading terms in a Taylor series expansion of the right-hand side of (50). The approximations used are identical with those used in deriving the Gaussian approximation to $W(X, Y)$, (47). There is no point in seeking any more accuracy in representing ν. All the expansions that are used depend upon the expansion of either R or $1/R$,

$$R = \sqrt{H^2 + X^2 + Y^2} = \frac{H}{S}\left[1 + CS\left(\frac{X}{H} - \frac{C}{S}\right) + \frac{S^4}{2} \cdot \left(\frac{X}{H} - \frac{C}{S}\right)^2 + \frac{S^2}{2}\left(\frac{Y}{H}\right)^2 + \cdots\right] \tag{51}$$

$$\frac{1}{R} = \frac{S}{H}\left[1 - CS\left(\frac{X}{H} - \frac{C}{S}\right) - S^2 \cdot \left(\frac{S^2}{2} - C^2\right)\left(\frac{X}{H} - \frac{C}{S}\right)^2 - \frac{S^2}{2}\left(\frac{Y}{H}\right)^2 + \cdots\right], \tag{52}$$

where we have used the notation

$$S = \sin\theta \tag{53}$$

$$C = \cos\theta. \tag{54}$$

Use of (51) in (50) then shows that

$$\nu = \frac{f_0}{c}[V_x S^3 + V_z C S^2]\left(\frac{X}{H} - \frac{C}{S}\right) + \frac{f_0}{c} V_y S \frac{Y}{H} + \cdots \text{(higher order terms)}. \tag{55}$$

To be consistent with the approximations to R involved in the steepest descent approximations used to derive (47) we neglect the higher order terms in (55). Then ν regarded as a random variable is represented as the linear combination of two independent zero mean Gaussian random variables. It follows from elementary statistics that ν will also be a zero mean Gaussian random variable with variance equal to the sum of the variances of the individual random variables. Thus the Doppler power spectrum is

$$P(\nu) = \frac{\sqrt{2}}{B_{\text{rms}}\sqrt{\pi}} \exp\left[-\frac{2\nu^2}{B_{\text{rms}}^2}\right], \tag{56}$$

where we have defined the rms Doppler spread as twice the standard deviation,

$$B_{\text{rms}} = 4\left(\frac{f_0}{c}\right)\alpha\sqrt{(V_x \sin\theta + V_z \cos\theta)^2 + V_y^2 \sin^2\theta}. \tag{57}$$

The time correlation function $p(\tau)$ is the Fourier transform of (56),

$$p(\tau) = \exp\left[-\tfrac{1}{2}(\pi\tau B_{\text{rms}})^2\right]. \tag{58}$$

Mallinckrodt computed $P(\nu)$ for airplane motion in the X direction (i.e., $V = (V_x, 0, 0)$ and in the Y direction ($V = (0, V_y, 0)$). For these special cases $P(\nu)$ in (56) agrees with Mallinckrodt's results (note that his $s = \sigma/L = \alpha\sqrt{2}$ and fix typos which left out $\sqrt{2}$ on [28, p. 27]). Staras [25] computed $p(\tau)$ for the cases of motion in the direction of each coordinate axis, i.e., $(V_x, 0, 0)$, $(0, V_y, 0)$, $(0, 0, V_z)$. Our result (58) when specialized to these cases agrees with his calculations for the two cases $V = (V_x, 0, 0)$ and $V = (0, 0, V_z)$. For airplane motion in the Y direction, however, his results differ

[11] Since the sea surface is moving this is clearly an approximation (to be included among all the others). However one may show that little error can be introduced in the estimate of $P(\nu)$, $Q(\xi)$, and $S(\xi, \nu)$ by this approximation in airplane communication channels.

from ours. The reason for the difference may be shown to be equivalent to the inclusion of the second-order term $(\sim Y(X-(C/S)H))$ in the Taylor expansion of Y/R in (50) about the specular point $Y=0$, $X=(C/S)H$. If the steepest descent argument is valid, the inclusion of this second-order term will yield different but not necessarily better approximations to the exact $p(\tau)$.

We consider now the computation of the delay power spectrum. From the geometry in Fig. 4 one may determine that the delay of a scattered signal from an area element at X, Y relative to the delay of scattered signals from the specular direction is given by

$$\xi = (1/c)\left(\sqrt{H^2+X^2+Y^2} - X\cos\theta - H\sin\theta\right). \quad (59)$$

Using (51) it is found that

$$\xi = \frac{H}{C}\frac{\sin\theta}{2}\left(\sin^2\theta\left(\frac{X}{H} - \operatorname{ctn}\theta\right)^2 + \frac{Y^2}{H^2}\right) + \cdots \text{higher order terms.} \quad (60)$$

Neglecting the higher order terms we see that the path delay ξ, regarded as a random variable, may be expressed as the sum of squares of two independent zero-mean Gaussian random variables. The density function and characteristic function of such a random variable are readily computed in closed form. The results are

$$Q(\xi) = \frac{1}{4\alpha^2 H/c}\exp\left(-\left[\frac{\sin\theta + 1/\sin\theta}{8\alpha^2 H/c}\right]\xi\right) I_0\left(\left[\frac{\frac{1}{\sin\theta} - \sin\theta}{8\alpha^2 H/c}\right]\xi\right) \quad (61)$$

$$q(\Omega) = \overline{\exp(-i2\pi\Omega\xi)} = \frac{1}{\sqrt{\left[1 + i4\pi\Omega\left(\frac{2H}{c}\frac{\alpha^2}{\sin\theta}\right)\right]\left[1 + i4\pi\Omega\left(\frac{2H}{c}\alpha^2\sin\theta\right)\right]}}, \quad (62)$$

which provide the normalized delay power spectrum and frequency correlation function of the diffuse channel (referenced to the specular path delay). Aside from a factor of $1/\pi$ in front and a scale factor on ξ, the $Q(\xi)$ computed by Mallinckrodt [28, eq. (26)] is the same as (61). Also Staras [25] has obtained the result (62), (complete the integration in his eq. (23a)). Plots of $Q(\xi)$ and $q(\Omega)$ as a function of the normalized variable $\xi/4\alpha^2(H/c)$ and $\Omega 4\alpha^2(H/c)$ are presented in Figs. 5 and 6 for several elevation angles.

The time-frequency correlation function of the channel is just the joint characteristic function of the random variables, ξ, ν. Thus

$$R(\Omega,\tau) = \overline{\exp(-i2\pi\Omega\xi)\exp(i2\pi\tau\nu)}, \quad (63)$$

where ξ, ν are given in terms of the X, Y variables. It is convenient to deal with normalized variables

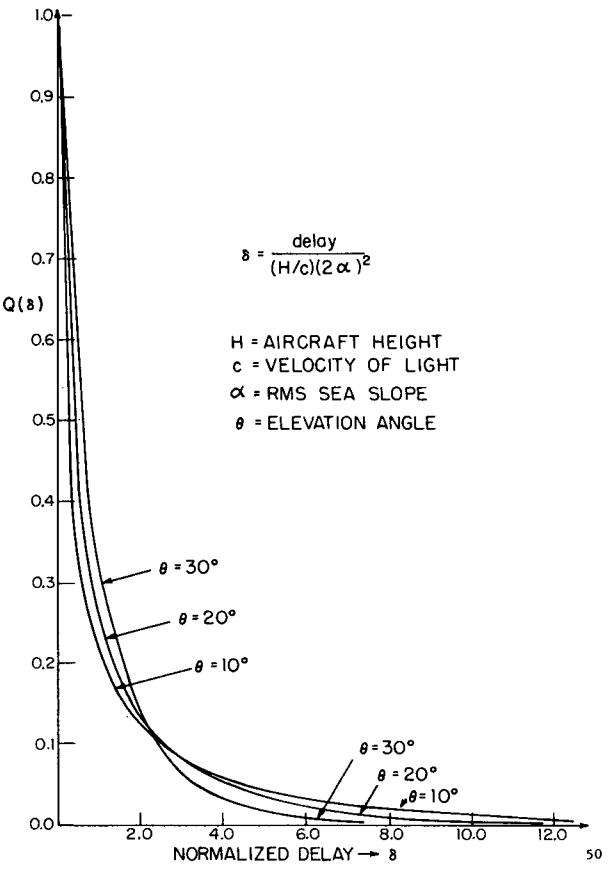

Fig. 5. Delay power spectrum for diffuse scatter.

$$\delta = \frac{\xi}{4\alpha^2 H/c} \quad (64)$$

$$\omega = \frac{\nu}{2\alpha} \quad (65)$$

$$x = \frac{\sin^2\theta}{2\alpha}\left(\frac{X}{H} - \operatorname{ctn}\theta\right) \quad (66)$$

$$y = \frac{1}{2\alpha}\cdot\frac{Y}{H}. \quad (67)$$

The variables x, y are zero-mean Gaussian with unit variances. In terms of normalized variables (55) and (60) show that

$$\delta = \frac{\sin\theta}{2}\left(\frac{x^2}{\sin^2\theta} + y^2\right) \quad (68)$$

$$\omega = \nu_\theta x + \nu_y \sin\theta\, y \quad (69)$$

where

$$\nu_\beta = (f_0/c)\, V_\beta \quad (70)$$

is the Doppler shift as measured along an axis in the β direction (ν_θ is the direct path Doppler shift $\nu_x \sin\theta + \nu_z \cos\theta$).

Consistent with the normalizations (64), (65) we used the

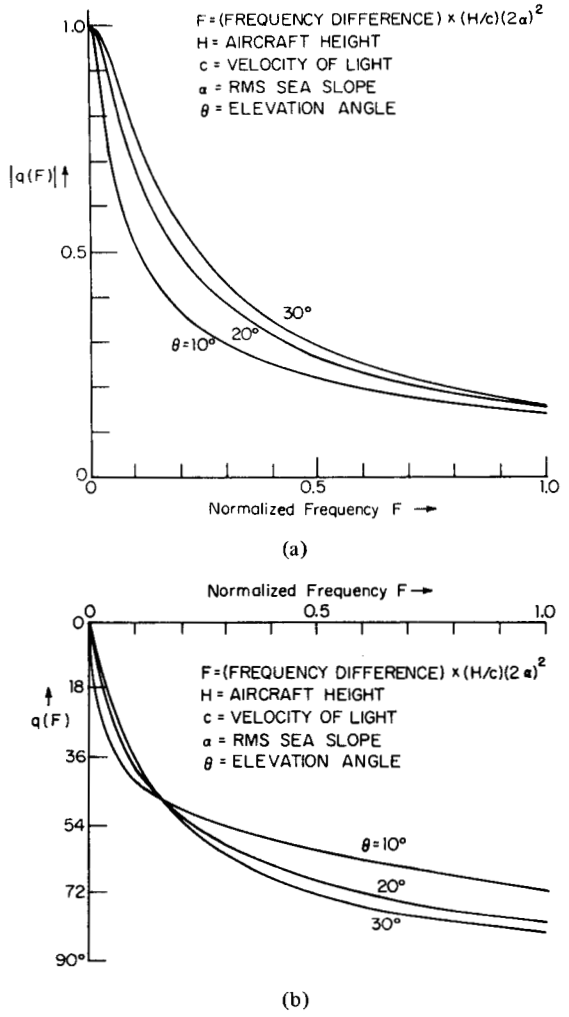

Fig. 6. (a) Magnitude of frequency correlation function for diffuse scatter. (b) Angle of frequency correlation function for diffuse scatter.

normalized shift variable

$$F = \Omega 4\alpha^2 H/c \tag{71}$$

$$T = \tau 2\alpha. \tag{72}$$

Then (63) becomes

$$R_0(F, T) = \overline{\exp(-i2\pi F\delta)\exp(i2\pi T\omega)}. \tag{73}$$

If (68) is used in (73) it is trivial to show that

$$R_0(F, T) = q_0(F)\exp\left(-\frac{1}{2}(\pi T)^2 \cdot \left[\frac{\nu_\theta^2}{1 + i2\pi F/\sin\theta} + \frac{\nu_y^2 \sin^2\theta}{1 + i2\pi F\sin\theta}\right]\right), \tag{74}$$

where

$$q_0(F) = 1/\sqrt{(1 + i2\pi F/\sin\theta)(1 + i2\pi F\sin\theta)} \tag{75}$$

is the frequency correlation function for the normalized variable.

The Fourier transform of $R(\Omega, \tau)$ along the τ axis $P(\Omega, \nu)$ is the cross power spectral density between two received carriers separated by Ω hertz in frequency. This function is of direct interest in the evaluation of tone ranging systems where range estimates depend upon the phase difference between filtered sidebands spaced in frequency. The Fourier transform is readily carried out to yield (in normalized variables)

$$P_0(F, \omega) = \sqrt{\frac{2}{H}}\, 1/\sqrt{\nu_\theta^2 + \nu_y^2\sin^2\theta + i2\pi F\sin\theta(\nu_\theta^2 + \nu_y^2)} \cdot \exp\left[-2\omega^2\left(\frac{[1 + i2\pi F/\sin\theta][1 + i2\pi F\sin\theta]}{\nu_\theta^2 + \nu_y^2\sin^2\theta + i2\pi F\sin\theta(\nu_\theta^2 + \nu_y^2)}\right)\right]. \tag{76}$$

To obtain the scattering function one may Fourier transform $P_0(F, \omega)$ along the F axis or, more simply, regard δ, ω as new random variables related to the variables x, y, by (68) and (69). Note that for each pair δ, ω there can be as many as two pairs of x, y values $(x_1(\delta, \omega), y_1(\delta, \omega)), (x_2(\delta, \omega), y_2(\delta, \omega))$, which satisfy these equations. Since the Jacobian of this transformation is given by

$$J(\delta, \omega) = \frac{\partial x}{\partial\delta}\frac{\partial y}{\partial\omega} - \frac{\partial y}{\partial\delta}\frac{\partial x}{\partial\omega} \tag{77}$$

the density function $S_0(\delta, \omega)$ is given in terms of $W_0(x, y)$, the density function of x, y, by

$$S_0(\delta, \omega) = J(\delta, \omega)[W_0(x_1(\delta, \omega), y_1(\delta, \omega)) + W_0(x_2(\delta, \omega), y_2(\delta, \omega))]. \tag{78}$$

We present the general expression for $S_0(\delta, \omega)$ in the Appendix. For the velocity vector in the XZ plane ($\nu_\theta \neq 0$, $\nu_y = 0$) one readily finds that

$$S_0(\delta, \omega) = \frac{1}{\pi\nu_\theta\sin\theta}\frac{1}{\sqrt{\frac{2\delta}{\sin\theta} - \frac{\omega^2}{\nu_\theta^2\sin^2\theta}}} \cdot \exp\left(\frac{\omega^2}{2\nu_\theta^2\tan^2\theta} - \frac{\delta}{\sin\theta}\right), \quad \omega^2 < 2\delta\sin\theta\,\nu_\theta^2. \tag{79}$$

For the velocity vector along the y axis $S_0(\delta, \omega)$ has the same form as (79) with ν_θ replaced by ν_y. For the general velocity vector it is rather more involved, as shown in the Appendix. Note that $S_0(\delta, \omega)$ in (79) vanishes for $\omega^2 > 2\delta\nu_\theta^2\sin\theta$ and becomes infinite at $\omega^2 = 2\delta\nu_\theta^2\sin\theta$. More generally, the Appendix shows that $S_0(\delta, \omega)$ vanishes for $\omega^2 > 2\delta(\nu_\theta^2 + \nu_y^2)\sin\theta$ and becomes infinite for $\omega^2 = 2\delta(\nu_\theta^2 + \nu_y^2)\sin\theta$. Expressions differing from (70) only by multiplicative constants and scale factors have been derived by Mallinckrodt [24], [28] for the velocity vector in the X or Y direction.

Channel correlation functions are particularly useful when they lead to a more complete statistical description of the channel as the case of the complex Gaussian WSSUS channel. To explain simply the conditions leading to Gaussian statistics

(the discussion may be made rigorous) we note heuristically that a transmitted signal of bandwidth W cannot resolve path delays less than $1/W$ apart. The locus of surface scatterers causing channel path delays lying between ξ and $\xi + 1/W$ is an elliptical ring. If the surface area of the ring extends over a large enough surface area to encompass many correlation lengths of the surface fluctuations, then, via central-limit-theorem-type arguments (and representation of the channel as a tapped delay line for a bandlimited signal [1], [34]), one may argue that the channel will act upon the input signal as if it were a Gaussian WSSUS channel. Moreover, as DeRosa has shown [5] the roughness condition $g^2 >> 1$ leads to the satisfaction of the symmetry conditions required for the complex Gaussian property. The bandwidth at which the Gaussian WSSUS property breaks down appears to be much larger than needed in aeronautical communications, at least when the roughness condition is valid.

There exist only a few measurements for airplane-satellite channels, and essentially only at UHF-VHF [35]-[41]. Generally speaking the measurements are not sufficiently detailed to provide the basis for checking the multipath and Doppler spread theories described above. Moreover, very little sea state measurements were taken in conjunction with the tests. However the measurements seem to check the theory in a gross way with regard to strength of the ground return and Doppler spread. Recent measurements at L band are reported in this issue [42], [43].

IV. Conclusion

The analytic expressions for channel correlation functions presented previously were derived under a restricted set of conditions:

1) one terminal so far from the earth that rays to the other terminal and glistening zone appear parallel;
2) elevation angle to far-terminal $\theta >>$ rms surface slope α;
3) roughness criterion $(4\pi\sigma \sin\theta/\lambda)^2 >> 1$;
4) small surface curvature for validity of Kirchhoff method $4\pi r_c \sin\theta/\lambda << 1$, where r_c is radius of curvature of surface;
5) no wave shadowing or multiple scattering effects.

Restrictions 1)-3) can be eliminated by using more general scattering cross-section formulas with more general geometry. But due to the complexity involved a computer is needed to obtain channel correlation functions. The simplest general results may be obtained for the scattering function because it involves only the computation of the Jacobian of the transformation from surface coordinates to delay-Doppler coordinates. Such general results have been programmed by DeRosa [5] for a composite surface model for general terminal positions and a spherical earth.

Restrictions 4) and 5) cannot be readily relaxed by existing analytical approaches. Clearly at low enough grazing and elevation angles 4) and 5) will become violated. Unfortunately low grazing angles are of considerable interest because of the reduced multipath discrimination provided by the nominally hemispherical coverage antennas proposed for use on air-traffic control systems. Thus the need for channel characterization experiments is clearly indicated in order to gather necessary data for system design.

Acknowledgment

The author would like to acknowledge the benefit of helpful discussions with his colleague Dr. J. K. DeRosa and thank Dr. Karp and L. Frasco of the Department of Transportation, Transportation Systems Center for reading and commenting on the manuscript.

Appendix

Scattering Function for General Velocity Vector

The scattering function for a general velocity vector is most easily derived by defining new variables

$$t = \frac{x}{S}\cos\Phi + y\sin\Phi \tag{A.1}$$

$$r = -\frac{x}{S}\sin\Phi + y\cos\Phi, \tag{A.2}$$

where $S = \sin\theta$ and

$$\nu_y/\nu_\theta = \tan\Phi. \tag{A.3}$$

In terms of these new variables the normalized delay and Doppler shift variables are

$$\delta = (S/2)[t^2 + r^2] \tag{A.4}$$

$$\omega = S\sqrt{\nu_y^2 + \nu_\theta^2}\, t. \tag{A.5}$$

Using the random variable interpretation of x, y as zero mean unit variance Gaussian variables, t and r become zero mean correlated variables with joint density function

$$W_1(t,r) = \frac{1}{2\pi\sigma_t\sigma_r\sqrt{1-\rho^2}} \exp\left\{-\frac{1}{2(1-\rho^2)} \cdot\left(\frac{t^2}{\sigma_t^2} + \frac{r^2}{\sigma_r^2} - \frac{2\rho rt}{\sigma_r\sigma_t}\right)\right\} \tag{A.6}$$

where

$$\sigma_t^2 = \frac{\nu_\theta^2/S^2 + \nu_y^2}{\nu_y^2 + \nu_\theta^2} \tag{A.7}$$

$$\sigma_r^2 = \frac{\nu_y^2/S^2 + \nu_\theta^2}{\nu_y^2 + \nu_\theta^2} \tag{A.8}$$

$$\rho = \frac{-\cos^2\theta\,\nu_y\nu_\theta}{\sqrt{(\nu_\theta^2 + S^2\nu_y^2)(\nu_y^2 + S^2\nu_\theta^2)}}. \tag{A.9}$$

The Jacobian of the transformation between δ, ω and t, r is quickly found to be

$$J(\delta,\omega) = \frac{1}{S\sqrt{\nu_y^2+\nu_\theta^2}\ \sqrt{\dfrac{2\delta}{S} - \dfrac{\omega^2}{S^2(\nu_y^2+\nu_\theta^2)}}}. \tag{A.10}$$

Note that for each ω, δ there are two pairs of values t, r:

$$t = \frac{\omega}{S^2\sqrt{\nu_y^2+\nu_\theta^2}} \quad r = \pm\sqrt{\frac{2\delta}{S} - \frac{\omega^2}{S^2(\nu_y^2+\nu_\theta^2)}}. \tag{A.11}$$

It follows that the scattering function

$$S_0(\delta, \omega) = J(\delta, \omega)\left\{W_1\left(\frac{\omega}{S\sqrt{\nu_y^2+\nu_\theta^2}}, \sqrt{\frac{2\delta}{S}-\frac{\omega^2}{S^2(\nu_y^2+\nu_\theta^2)}}\right) + W_1\left(\frac{\omega}{S\sqrt{\nu_y^2+\nu_\theta^2}}, -\sqrt{\frac{2\delta}{S}-\frac{\omega^2}{S^2(\nu_y^2+\nu_\theta^2)}}\right)\right\}, \quad \text{(A.12)}$$

where $J(\delta, \omega)$ is given by (A.10) and $W_1(t, r)$ is given by (A.6) with the parameters (A.7)–(A.9).

References

[1] P. A. Bello, "Characterization of random time-variant linear channels," *IRE Trans. Commun. Syst.*, vol. CS-11, pp. 360–393, Dec. 1963.

[2] J. L. Doob, *Stochastic Processes.* New York: Wiley, 1953.

[3] R. Arens, "Complex processes for envelopes of normal noise," *IRE Trans. Inform. Theory*, vol. IT-3, pp. 204–207, Sept. 1957.

[4] P. A. Bello, "A study of the relationship between multipath distortion and wavenumber spectrum of refractive index in radio links," *Proc. IEEE*, vol. 59, pp. 47–75, Jan. 1971.

[5] J. K. DeRosa, "The characterization of multipath and Doppler fading in earth scatter communication, navigation and radar links," Ph.D. dissertation, Northeastern Univ., Boston, Mass., June 1972.

[6] P. Beckmann and A. Spizzichino, *The Scattering of Electromagnetic Waves From Rough Surfaces.* New York: Pergamon, 1963.

[7] C. Cox and W. Munk, "Statistics of the sea surface derived from sun glitter," *J. Marine Res.*, vol. 13, no. 2, pp. 195–227, 1954.

[8] L. M. Brekhovskikh, "The diffraction of waves by a rough surface, part I" (in Russian), *Zh. Eksp. Teor. Fiz.*, vol. 23, pp. 275–289, 1952.

[9] T. Hagfors, "Scattering and transmission of electromagnetic waves at a statistically rough boundary between two dielectric media," in *Electromagnetic Wave Theory Part II*, J. Brown, Ed. New York: Pergamon, 1966.

[10] A. Stogryn, "Electromagnetic scattering from rough, finitely conducting surfaces," *Rad. Sci.*, vol. 2, Apr. 1967.

[11] D. E. Barrick, "Relationship between slope probability density function and the physical optics integral in rough surface scattering," *Proc. IEEE* (Lett.), vol. 56, pp. 1728–1729, Oct. 1968.

[12] B. Semenov, "Scattering of electromagnetic waves from restricted portions of rough surfaces with finite conductivity," *Radiotekh. Elektron.*, vol. 68, no. 11, pp. 1952–1960, 1965.

[13] R. D. Kodis, "A note on the theory of scattering from an irregular surface," *IEEE Trans. Antennas Propagat.*, vol. AP-14, pp. 77–82, Jan. 1966.

[14] J. A. Stratton, *Electromagnetic Theory.* New York: McGraw-Hill, 1941.

[15] P. Horn *et al.*, "Theoretical study of multipath effects in an aeronautical satellite system," Messerschmidt-Bialkow Blohm GmbH for European Space Res. Technol. Cen., Syst. Study Div., Noordwijk, Holland, Final Rep. Contr. 1064/70CG (RFQ 1737).

[16] D. E. Kerr, *Propagation of Short Radio Waves.* New York: Dover, 1965.

[17] N. W. Guinard and J. C. Daley, "An experimental study of a sea clutter model," *Proc. IEEE*, vol. 58, pp. 543–550, Apr. 1970.

[18] S. O. Rice, "Reflection of electromagnetic waves by slightly rough surfaces," *Commun. Pure Appl. Math.*, vol. 4, pp. 361–378, Feb./Mar. 1951.

[19] J. W. Wright, "A new model for sea clutter," *IEEE Trans. Antennas Propagat.*, vol. AP-16, pp. 217–223, Mar. 1968.

[20] G. R. Valenzuela, "Scattering of electromagnetic waves from a tilted slightly rough surface," *Rad. Sci.*, vol. 3, Nov. 1968.

[21] I. M. Fuks, "Theory of radio wave scattering at a rough sea surface," *Izv. Vyssh. Uchef. Zaved. Radiofiz.*, vol. 9, no. 5, pp. 876–887, 1966.

[22] a. F. G. Bass, I. M. Fuks, A. I. Kalmykov, I. E. Ostrovsky, and A. D. Rosenberg, "Very high frequency radiowave scattering by a disturbed sea surface, part I: Scattering from a slightly disturbed boundary," *IEEE Trans. Antennas Propagat.*, vol. AP-16, pp. 554–559, Sept. 1968.
b. —, "Very high frequency radiowave scattering by a disturbed sea surface, part II: Scattering from an actual sea surface," *ibid.*, pp. 560–568.

[23] C. T. Swift, "A note on scattering from a slightly rough surface," *IEEE Trans. Antennas Propagat.*, vol. AP-19, pp. 561–562, July 1971.

[24] A. J. Mallinckrodt, "Ground multipath in satellite-aircraft propagation," presented at the Symp. Application of Atmospheric Studies to Satellite Transmissions, Boston, Mass., Sept. 1969.

[25] H. Staras, "Rough surface scattering on a communication link," *Rad. Sci.*, vol. 3 (new series), pp. 623–631, June 1968.

[26] S. H. Durrani and H. Staras, "Multipath problems in communication between low-altitude spacecraft and stationary satellites," *RCA Rev.*, pp. 77–105, Mar. 1968.

[27] J. K. DeRosa, "On the determination of the delay-Doppler scattering function for a ground-to-aircraft link," presented at the 1970 Can. Symp. Communications, Nov. 12–13, 1970.

[28] A. J. Mallinckrodt, "Propagation errors," Notes for UCLA Short Course, *Satellite Based Navigation Traffic Control and Communications to Mobile Terminals*, Sept. 14–25, 1970.

[29] L. H. Ford and R. Oliver, "An experimental investigation of the reflection and absorption of 9 cm wavelength," *Proc. Phys. Soc.*, vol. 58, p. 265, 1946.

[30] J. S. McPetrie, "The reflection coefficient of the earth's surface for radio waves," *Proc. Inst. Elec. Eng.* (London), vol. 82, p. 214, 1938.

[31] K. Bullington, "Reflection coefficients of irregular terrain," *Proc. IRE*, vol. 42, pp. 1258–1262, Aug. 1954.

[32] C. I. Beard, I. Katz, and L. M. Spetner, "Phenomenological vector model of microwave reflection from the ocean," *IRE Trans. Antennas Propagat.*, vol. AP-4, pp. 162–167, Apr. 1956.

[33] R. E. McGavin and L. J. Maloney, "Study at 1.046 Mc/s of the reflection coefficient of irregular terrain at grazing angle," *J. Res. Nat. Bur. Stand.*, vol. 63D, pp. 235–248, 1959.

[34] T. Kailath, "Sampling models for linear time-variant filters," M.I.T. Res. Lab. Elec., Cambridge, Mass., Rep. 352, May 1959.

[35] G. Bergmann and H. Kucers, "Signal characteristics of a VHF satellite-to-aircraft communication link for 30 to 70 degree elevation angles," Collins Rad. Co., 523-0759781-00 181M, Oct. 14, 1967.

[36] K. L. Jordan, Jr., "Measurement of multipath effects in a satellite-aircraft UHF link," *Proc. IEEE* (Lett.), vol. 55, pp. 1117–1118, June 1967.

[37] I. I. Foshee and G. E. LaVean, "Multipath and propagation experiment utilizing VHF/UHF satellite communication system," AIAA Paper 68-419, Apr. 1968.

[38] G. W. Leopard, "The flight evaluation of aircraft antennas," *IRE Trans. Antennas Propagat.*, vol. AP-8, pp. 158–166, Mar. 1960.

[39] W. M. Browne, "Propagation in the 960 to 1215 MHz range," NATC, Patuxent River, Md., Combined Final Rep., Proj. PTR EL 44012.3, 44012.4, Ser. ET 312-412, Oct. 1954.

[40] G. W. Leopard and W. S. Bartels, "NATC methods for flight evaluation of aircraft antennas," Final Rep. Proj. PTR AV 44009, Oct. 1958.

[41] A. L. Johnson and M. A. Miller, "Three years of airborne communication testing via satellite relay," Air Force Avionics Lab. Tech. Rep. AFAL-TR-70-156, Nov. 1970.

[42] R. W. Sutton, E. H. Schroeder, A. D. Thompson, and S. G. Wilson, "Satellite-aircraft multipath and ranging experimental resultant *L* band," this issue, pp. 639–647.

[43] J. Liv, J. Kramer, and S. Karp, "*L*-band multipath tests vol. I: Experiment design and CW tests," U.S. Dep. Transp., Transp. Syst. Cen., Cambridge, Mass., Aug. 1972.

Phillip A. Bello (S'52-A'55-M'60-SM'62-F'70) was born in Lynn, Mass., on October 22, 1929. He received the B.S.E.E. degree from Northeastern University, Boston, Mass., in 1953 and the S.M. and Sc.D. degrees in electrical engineering from the Massachusetts Institute of Technology, Cambridge, in 1955 and 1959, respectively.

From 1955 to 1957 he was an Assistant Professor of Communications at Northeastern University. He was an Engineering Specialist at Sylvania Applied Research Laboratory from 1958 to 1961 and a Senior Scientist of Adcom from 1961 to 1965. He was Vice President of Signatron, Inc., for seven years, where he was responsible for the company's research and development work in the communications area. Presently, he is President of CNR, Inc., Newton, Mass., a company devoted to research and development in communications and allied fields. In this position he both directs technical efforts and engages in the solution of detailed technical problems. His work includes both development and analysis of techniques for high-speed digital communications, nonlinear and linear communications channel simulation, and communications channel characterization for a wide variety of communications media.

Dr. Bello is a member of the International Scientific Radio Union, Commission VI.